HydroFracture Monitoring Using Vector Scanning With Surface Microseismic Data*

Quansheng Zhang[1], Zhanchun Ren[1], Bintao Zheng[1], Lei Wang[1], Shigang Yang[2], and Beiyuan Liang[3]

Search and Discovery Article #41459 (2014)
Posted October 6, 2014

*Adapted from extended abstract prepared for oral presentation at AAPG International Conference and Exhibition, Istanbul, Turkey, September 14-17, 2014

[1]Shengli Oil Field, China
[2]Zhongyuan Oil Field, China
[3]GeoImage LLC. Gainesville, Georgia (bjjywd@126.com)

Introduction

Since 2006, we have monitored hydrofracturing (HF) processes of over 100 oil/gas wells in sandstone, carbonate, shale, coal bed, etc. for developing a vector scanning method with microseismic data recorded on surface. Our purpose is to achieve a cost-effective detection routine for HF through surface network with sparsely distributed 3-component seismic stations, and near real time 3D imaging of the geometry of fractures in acceptable precision. Based on the method (Ma etc. 2012), this article describes important developments of it in the last two years.

Principle

Two critical features in HF exist:
1) They consist of numerous micro-fractures, so that the seismic events, in general, cannot be located by picking P and S wave arrivals (pPS) from surface records.
2) Besides the tensile fractures, shear rupturing is the most commonly encountered fractures (e.g., Zhu, et al., 1996; Rutledge et al., 2003; Eisner et al., 2010).

We have, therefore, to solve the three key problems:

A) Seismic stations should be about 1-2 km from the fracturing vehicles, and each station location must be quiet determined by a seismometer instead of a person. This kind of data acquisition is to avoid any strong noise from the vehicles, etc., and in fact, the total length of a curved seismic trace emitted from HF location to surface station is now similar to that of stations closer to the vehicles.
B) All seismic stations should be equipped with 3-component sensor, each of which should be screwed into ground for being well coupled with land. Every station should also be independently controlled by GPS, and it can transmit numerous real-time data wirelessly and quickly.
C) Instead of scalar stacking (semblance coefficient, Sheriff, 1991) or pPS for 4D imaging from the surface data, a vector stacking should be used.

$$S(k)= (\Sigma_i[\Sigma_j(\pm)(f_{ij})]2) /F, \qquad (1)$$

where S(k) is seismic energy emitting from kth point in a target volume; f_{ij} a vector at jth record sample of ith station; F, a chosen normalization factor; and the sign ± before f_{ij} is determined by the feature of shear rupturing, or the correlation between a reference station and the stacked station in a time window.

.

Data Acquisition

Except for the constraints from the features of HF and the vector scanning mentioned above, data acquisition should also satisfy the requirements from oil fields, such as a higher ratio of performance-cost, not any special limit and condition (e.g., suspended production, and/or an additional monitoring well), a quickly constructed seismic network so that the monitoring can be a routine work; real-time or near real-time processing and interpretation, etc. In addition, there may exist dense cable/pipe network s under or above ground, roads (vehicles), villages, oil/gas/water/drilling wells, fluid injecting, and complicated topography as monitoring environment.

The following conditions for our special seismic instruments should be and have been satisfied:
1) 3-component sensor screwed into ground for being well coupled with land;
2) Each is controlled by GPS independently without the limit from topography;
3) After determining 20-30 quiet points for stations in a square of more than 10 km^2 using a special prospecting instrument for background noise, the network can be quickly constructed in several hours on surface;
4) All parameters, including smaller sample interval and broad frequency band, should be suitable to microseismic monitoring;
5) A great number of data can be transmitted to a processing and interpretation center wirelessly in a speed of ≥GSM.

The cardinal principles of constructing the network in a survey are listed below and shown in Figure 1), based on the sequence of their importance:
A) Each seismograph can record and transmit data continuously and reliably;
B) All of seismographs should be at quiet locations, specially far away (at least 1km) from fracturing vehicles;
C) The network covers evenly the monitored target or region projected to surface.
There may be, thus, a variety of geometric distributions for the network, such as ring, elliptic ring, several small regions, even in a quadrant, etc.

An average amplitude, A, is defined to determine if a point is quiet or noisy based on our experiences in data processing and interpretation. For a 24-bit recorder with a gain of 340, and a seismometer with sensitivity of 400mV/cm/s, A is the percentage of the average amplitude(A) of 3 components relative to half of measurement range (2^{23}) , that is

$$A = 100 \times \frac{\bar{A}}{2^{23}} \quad . \qquad (2)$$

Table 1 shows the relationship between A and quality of data acquisition.

Note that there are two constraints:
a) If A >1, or even thoughA≤1 but the total number of quiet points <5-6,the project may not be performed;
b) Even though A≤1, if it is noisy from some machines with fixed frequencies, so called "bottle gourd", the point may not be used.

We can always find some quiet points or small regions in past projects (except for two with city environment, and desalination plant with gale, respectively), such that the quality constraint lays a solid foundation for processing and interpretation.

Data Processing and Interpretation

We have to process the seismic data based on, again, the HF features and Equation (1) described above, so that the processed data could satisfy random characteristics for stacking, and any record without relationship to HF ruptures will be removed or suppressed. After this king kind of processing, the relatively greater emit-energy from HF may be shown more clearly around the fracturing point of a well.
Our detailed and important approaches in data processing include, step by step:

1) Band pass of, for example, 1-45Hz, even 1-25Hz. Because monitored microseismic events are located at a depth of several hundreds to thousands of meters, the energy with higher frequencies in useful microseismic signals have been attenuated. This band pass will effectively remove a number of interferences from the surface.
2) Suppressing or removing variety of interference records without respect to fracturing ruptures, such as:

(a) moving vehicles, persons, and animals;

(b) natural earthquakes and man-made explosions;

(c) some kinds of machines with several fixed frequencies, so called "bottle gourd" in signals, even though the amplitudes of them look smaller.

Sometimes for the relatively larger earthquake records in (b), we should identify their aftershock interferences in a certain time interval. For any interference in (c), even with small amplitudes, we should remove it for it may occupy a dominant position in stacking. However, the processing step should not, as best as we can, damage the normally random signals because the smaller HF signals exist in them.
3) Removing the stations still with larger average amplitude after actions 1) and 2), because they may be dominant in stacking, even though we cannot temporarily find any reasonable interpretation for them.

All of the data processing and stacking described above are performed through automatically parallel background computation in a multi-core (i.e., 32-128) computer or any cloud computing, except for a final check for the data just before stacking for each time window (i.e., several to several hundreds of seconds). The progress can be real time or near real time together with areal fracturing process, or performed for all time intervals after fracturing. Figures 2 and 3 show a typical example in data processing and interpretation.

The example in Figure 2 is one of the most complicated intervals in processing. It includes almost all kinds of interferences from surface or natural earthquakes, and there are not many stations left, as we would expect. Of course, the stacking output will be better if we avoid the points with "bottle gourd" record in the field survey. Figure 2 shows also the analysis for each interference by our processing software and man's eyes. The150s interval is finally divided into two sub-intervals after removing the earthquake term. A validation for the data processing and scanning is shown in Figure 3 for the intervals.

In Figure 3, one can find that the energy-color scale in C is much higher than that in A and B; this means there are many effects of interferences from surface and possible far-removed earthquakes. However, sub-Figure 3A, after removing most of interferences, shows that our data processing produces prominent energy distribution around fracturing point (another sub-interval B may not have strong fracturing events) and a good base for interpretation.

Figure 3A shows, in fact, the features for the vector scanning output after good data survey and data processing: residual interferences do still exist but are not prominent; there are some higher energy spots or stripes, especially around fracturing point; the other spots or stripes with relatively lower energy values may be the effect of stacking periodic data. The features also are validated in our forward modeling (Ma et al., 2012) and other applications.

Stacking data using Equation (1) relies on a velocity model--and corresponding travel time and incident geometry tables between each pair of station and scanning point for whole target volume. This is an important base to stack data successfully. Therefore, one has to interpolate a velocity model as close as possible to a real one by using available sonic measurements and exploration outputs, even some of our own measurements. Making the velocity model should firstly construct a 3D curved surface or topography if the target region is a mountain or loess tableland. A geometrical design (Figure 1, middle left) consists of making velocity model, calculating travel time table, and determining correct positions of fracturing stages based on the deviated data of a well.

Applications

The proposed vector scanning method has also been applied to over 100 oil/gas wells, except for the examples mentioned above and in our forward modeling.

Figure 4 shows a validation of the vector scanning method using known production data, at that time Well B660-19 erupted when well B660-20 was being fractured.

Figures 5 and 6 and Table 2 show an application of the method for comparing our scanning as well as in a monitoring well which is close to the fracturing stage.

Figures 7 and 8 display the scanning outputs for a total of 86 stages in 9 horizontal wells in block Yan227 in Shengli oil field, and a summarized relationship between the interpreted fracture lengths and the injected volumes, respectively.

Conclusions

Our experiments suggest that the vector scanning is a cost-effective technique, which can be a routine performance together with normal HF processes. Like any new technical development, one has to carefully and strictly consider, study, test, and solve each detailed step or problem from, e.g., the features in HF, special instruments, field survey, scanning design, data processing, and interpretation, if its principle and feasibility are reasonable. Not to do so, one may easily give up or deny it, or get incorrect conclusion, even due to a tiny bit of trouble.

References Cited

Eisner L., P. Duncan, and M. Thornton, 2010, Beyond the dots in the box: Microseismicity-constrained fracture models for reservoir simulation: The Leading Edge, v. 29, p. 326-333.

Ma, L., Ll. Wang, Y. Shen, Y. Zhou,and B. Liang, 2012, Vector scanning: hydro-fracture monitoring with surface microseismic data: SPE-152913, Copenhagen, Denmark.

Rutledge J.T., and W. Phillips, 2003, Hydraulic simulation of natural fractures as revealed by induced micro-earthquakes, Carthage Cotton Valley gas field, east Texas: Geophysics, v. 68/2, p. 441-452.

Sheriff, R.E., 1991, Encyclopedic Dictionary of Exploration Geophysics, 3rd Edition: Society of Exploration Geophysicists, 376 p.

Zhu, X. H.J. Gibson, and N. Ravindran, 1996, Seismic imaging of hydraulic fractures in Carthage tight sands: A pilot study: The Leading Edge, v. 15, p. 218-224.

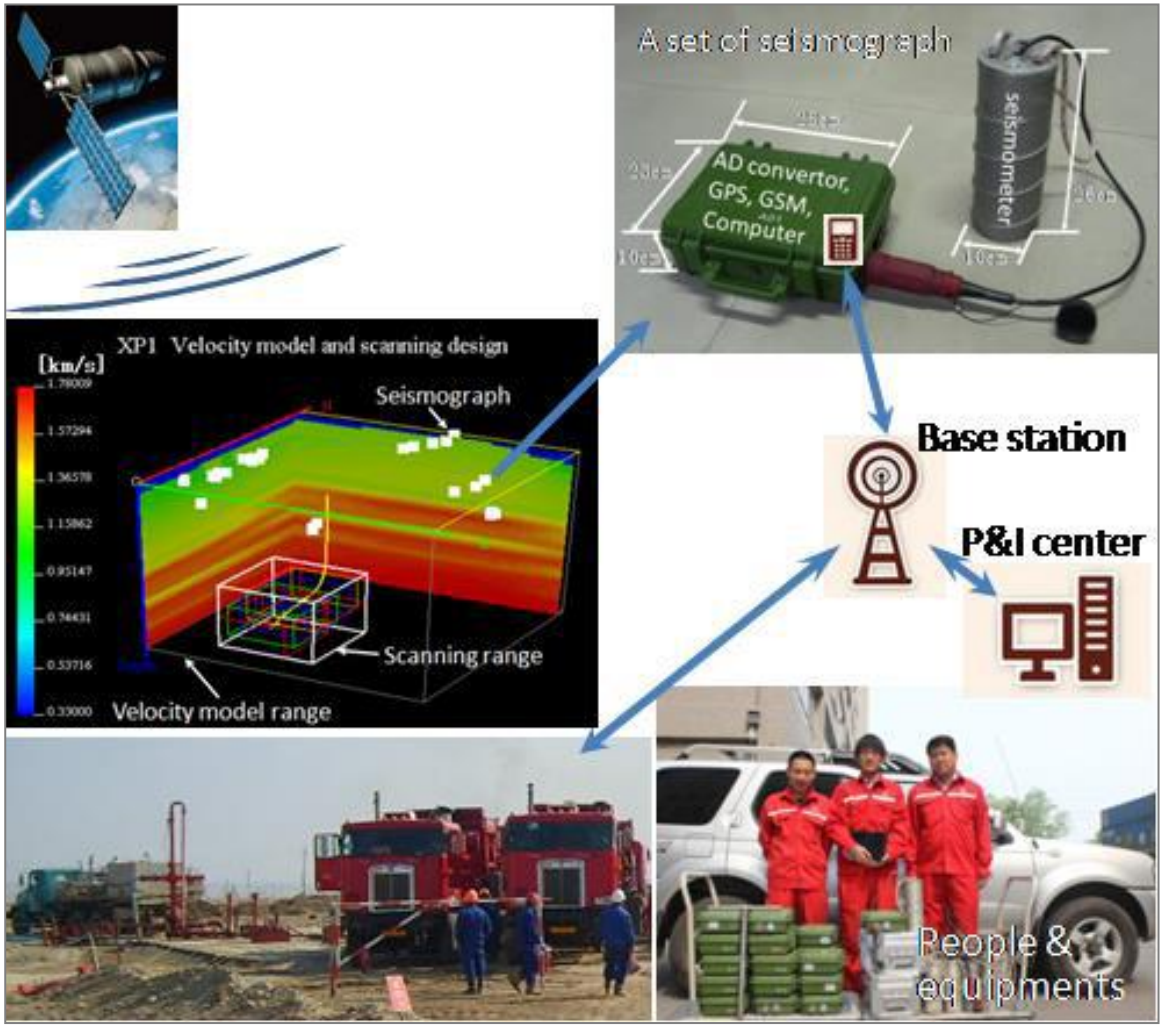

Figure 1. Our special instruments, seismic network, survey design, and people for data acquisition.

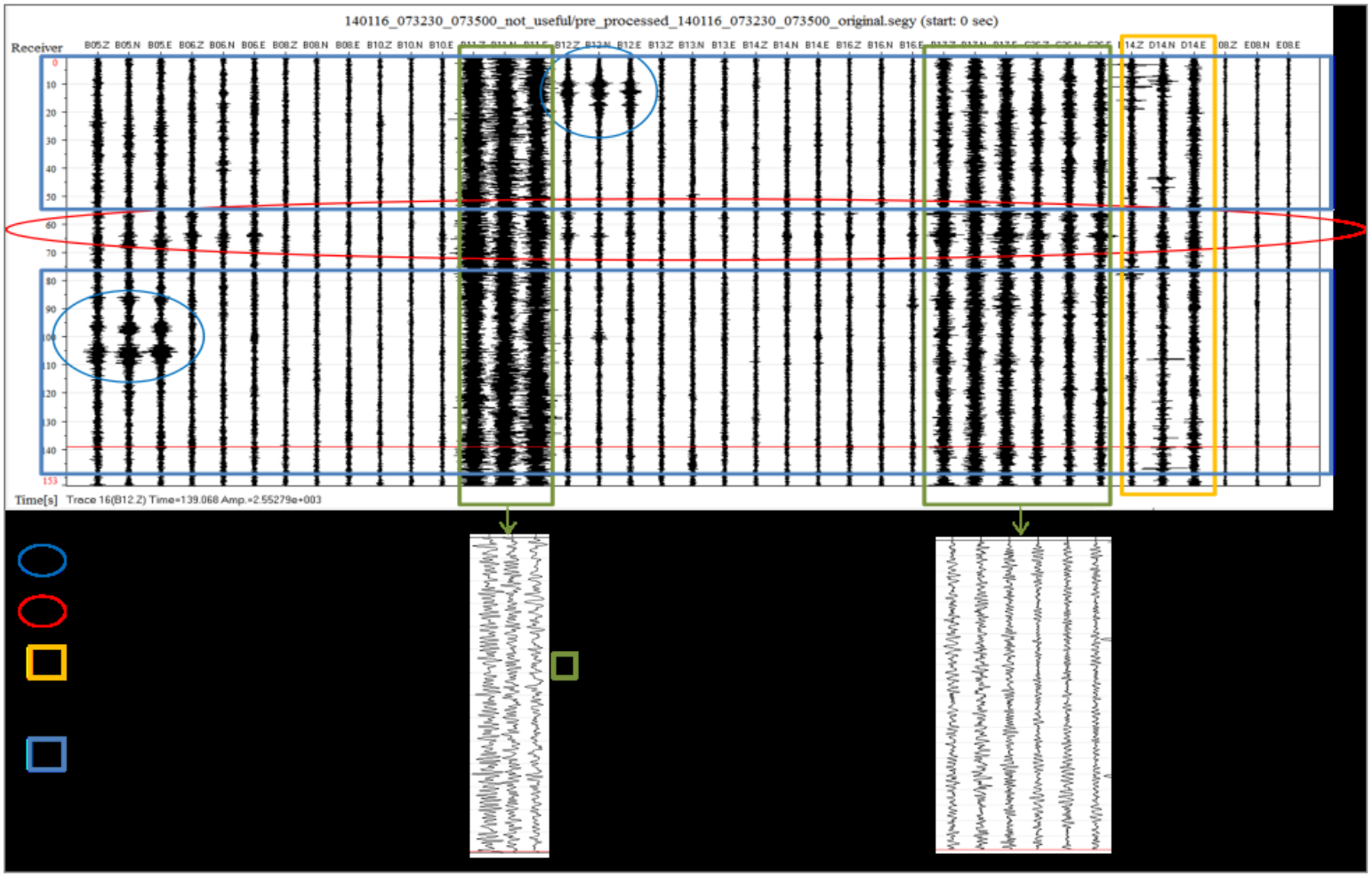

Figure 2. The original record of fracturing survey in a time interval of 150s for well XP1(stage 1). Except for the 13 stations in the figure, another 10 stations with "bottle gourd" records have been removed by the original processing software. Each station includes 3 traces in Z, north, and east directions, respectively. Horizontal axis is station sequence, and vertical one is time axis in seconds.

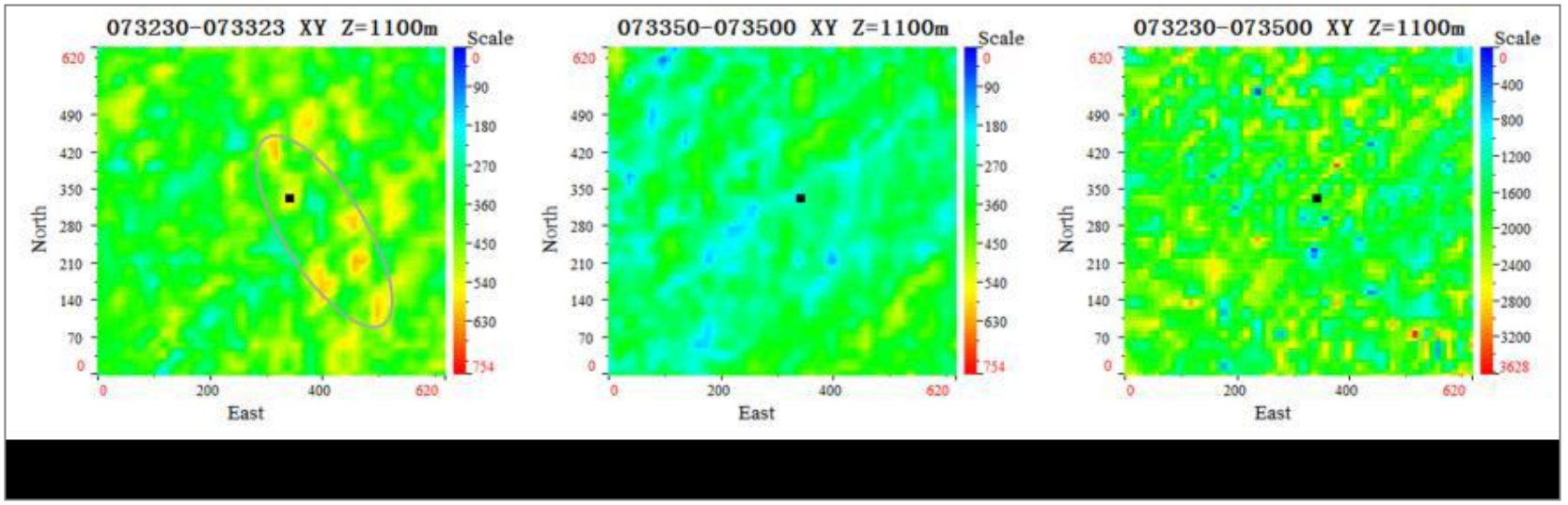

Figure 3. The validation of the vector scanning method using the processed (A and B) and unprocessed (C) data, corresponding to an original time interval (C) and its two sub-intervals (A and B), respectively, in Figure 2. Each is 2D fracture energy distributions of monitoring fracturing just at fracturing start. Horizontal axis is east and vertical axis is north with distance in meters. The small black square is the fracturing point. The gray ellipse in A shows the range of higher emitting energy corresponding to a possible fracture geometry.

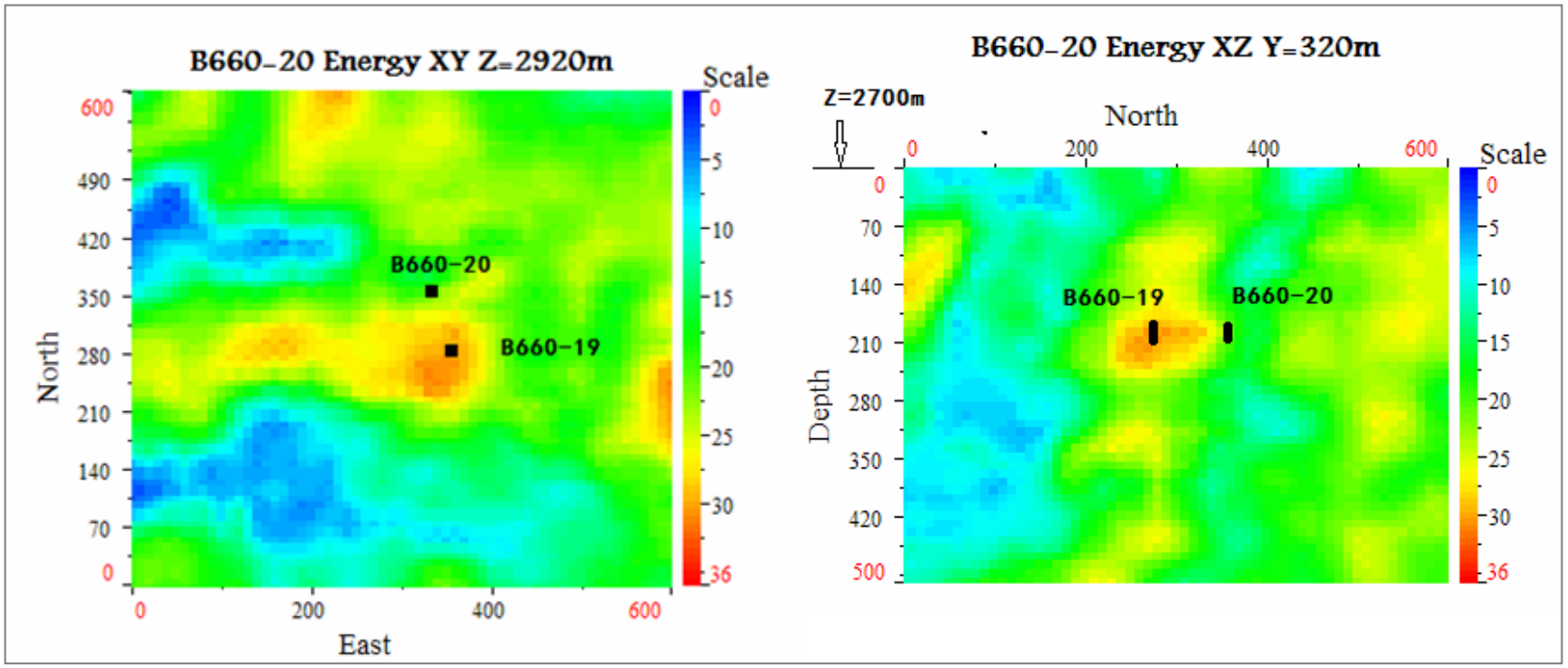

Figure 4: The validation of the vector scanning method using known production data. The 2D fracture energy distributions of monitoring fracturing for well B660-20. Left: horizontal plane at a depth of 2920 m. Right: vertical section across the wells. Black squares are the wells at the corresponding depths. Well B660-19 erupted when well B660-20 was being fractured. Both are vertical wells.

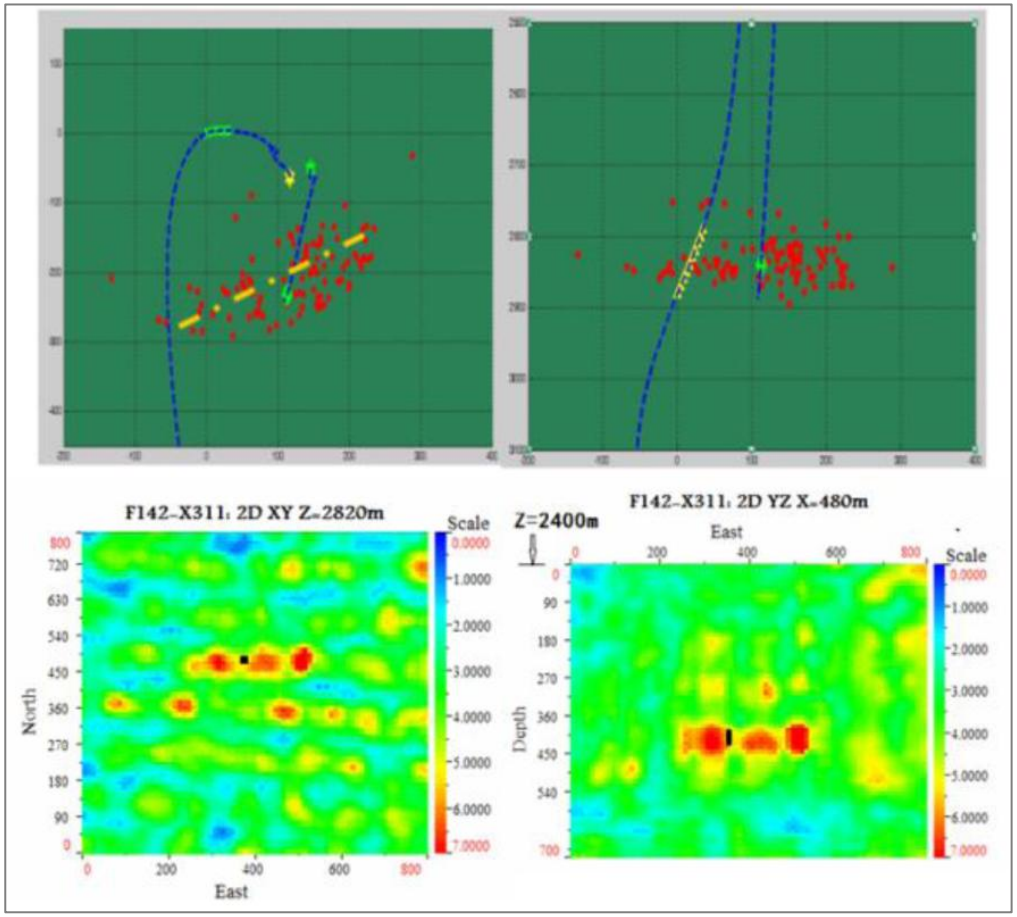

Figure 5. Comparison between the vector scanning (the bottom row with fracture energy distribution) and the seismic monitoring in a well and close to fracturing segment (the upper row with fracture points located), for well F142-X311 in Shengli oil field. The left image shows the fracture projection onto the horizontal plane; the right image shows the projection as a vertical cross-section oriented easterly. Both planes measured the HF, processed and interpreted independently. The outputs are tabulated and shown in Table 2.The scanning progress with respect to time is shown in Figure 6.

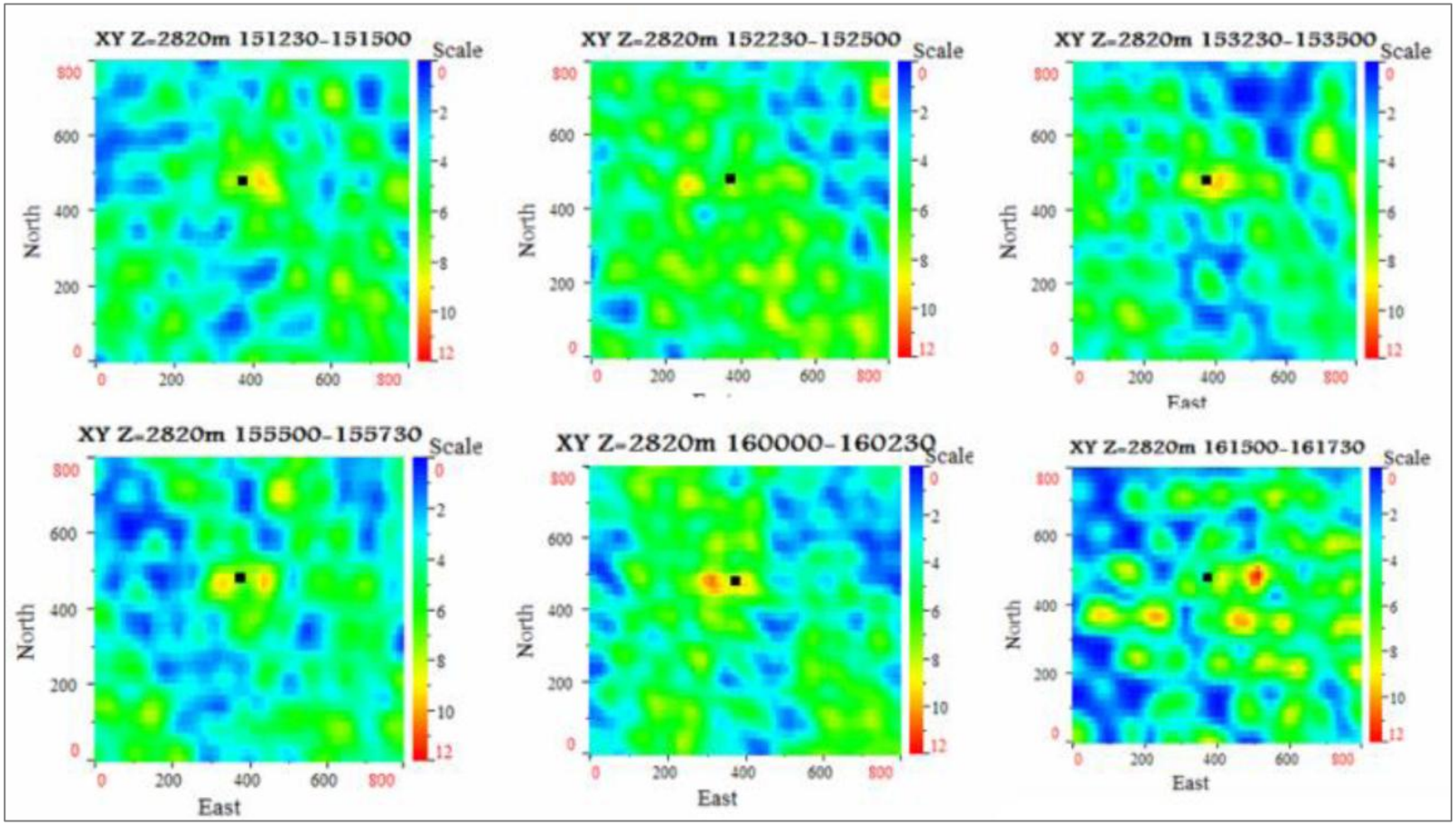

Figure 6. The scanning progress with respect to time shown in Figure 5 (bottom line plots). Here the only intervals with higher energy around the fracturing point are shown, and their combination is that shown in the bottom line of Figure 5.

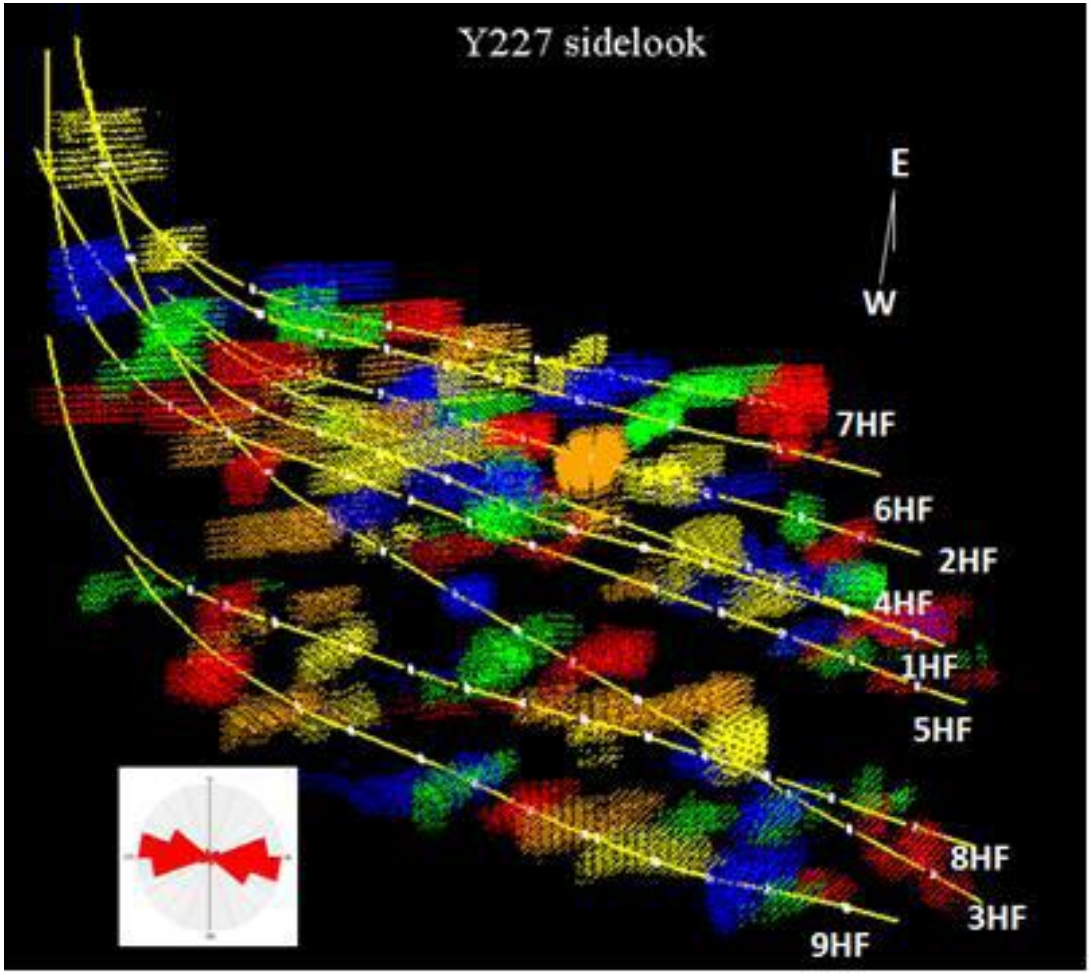

Figure 7. The application of vector scanning in HF for horizontal wells in block Y227. It is side-look distribution of the greater released fracturing energy for 9 wells. Well trajectories are displayed as yellow. The colored dots close to each stage (white point) show the high fracturing energy in 3D. The different colors shown here are only for identification among the stages. A sub-figure at lower left shows the statistical orientations of the all interpreted fractures.

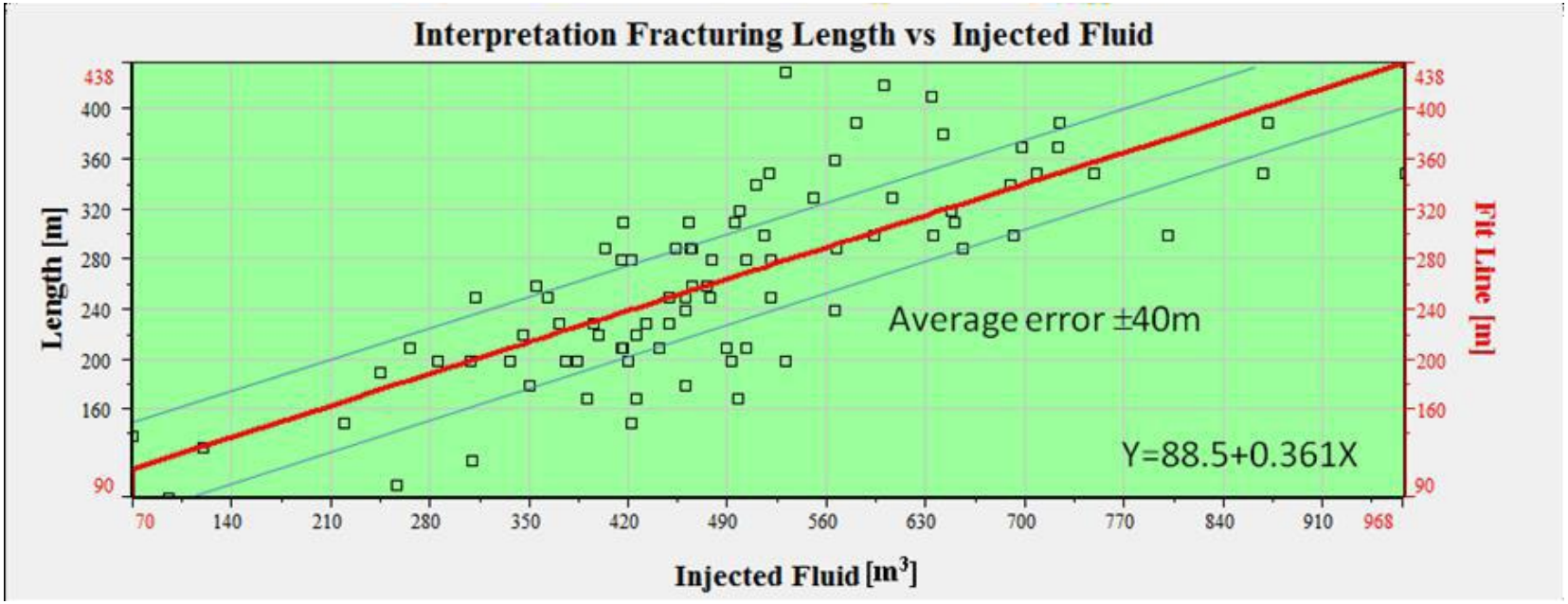

Figure 8. A relationship between the interpreted fracture lengths (black squares) and the injected volumes. A red line for fitting data shows a relationship between them. This relationship is significant for future HF, development of block Y227,and even possibly general sand-gravel reservoirs.

A （≤N%）	quality of data acquisition
1.00	Ok
0.75	Good
0.50	Perfect

Table 1. Quality of data acquisition using value A.

Methods	Orientation(degrees)	Length(m)	Geometry
Monitoring in a well	NE75	240	Symmetric two wings
Vector scanning on surface	NE85	200-300	Symmetric two wings

Table 2. Description of the HF in values corresponding to Figure 3.